HRMS SPECIAL ISSUE

High-resolution spectroscopic study of the H_2O-CO_2 van der Waals complex in the 2OH overtone range

C. Lauzin[a], A. C. Imbreckx[a], T. Foldes[b], T. Vanfleteren[b], N. Moazzen-Ahmadi[c] and M. Herman[b]

[a]Institute of Condensed Matter and Nanosciences, Université catholique de Louvain, 1348, Louvain-la-Neuve, Belgium.;
[b]Service de Chimie quantique et Photophysique, CP 160/09, Faculté des Sciences, Université Libre de Bruxelles, Brussels, Belgium.
[c]Department of Physics and Astronomy, University of Calgary, 2500 University Drive North West, Calgary, Alberta T2N 1N4, Canada

ARTICLE HISTORY
Compiled December 9, 2019

ABSTRACT
The jet-cooled spectrum (T_{rot} = 12K) of the H_2O-CO_2 van der Waals complex has been recorded in the 1.4 μm region by cavity ring-down spectroscopy. Two *b*-type vibrational bands have been observed and analysed. The rotational assignment has been achieved using a different asymmetric rotor Hamiltonian for each nuclear spin species, accounting for the internal rotation of the H_2O and CO_2 units. The band at 7247 cm^{-1} is assigned to (101) in terms of the (v_1 v_2 v_3) vibrational quantum number of the H_2O monomer. The band at 7238 cm^{-1} is assigned to (200) +an intermolecular mode (v_{12}) excited in the complex. Vibration-rotation constants are provided for the excited states. The symmetry of the wavefunction, the effect of vibrational excitation on the tunneling dynamics and the vibrational assignment are discussed.

KEYWORDS
van der Waals complexes, tunneling, cavity ring-down, combination band.

1. Introduction

The characterization of the interaction between H_2O and CO_2 is relevant for several fields of research. These species are the main greenhouse gases in the Earth atmosphere. These molecules are present in several atmospheres and the complexation with H_2O is considered as one scenario to account for observed shifts of the ν_3 band origin of CO_2 in different environments [1]. The possibility to store CO_2 in water chlatrates is currently a field of investigation theoretically [2] and experimentally [3]. H_2O-CO_2 has been studied in the literature. The microwave spectrum of this complex was first measured by Peterson and Klemperer using molecular beam electric resonance spectroscopy [4]. These measurements were later extended by Columberg *et al.* [5], where they studied a larger set of isotopologues and extended the number of observed transitions. These authors developed a specific Hamiltonian accounting

Email: clement.lauzin@uclouvain.be

for the relaxation of the intermolecular distance during the rotation of the complex. This Hamiltonian included also the low barrier potential of the relative internal rotation of the H_2O and CO_2 units. A value of 286.965 cm^{-1} for the barrier was determined by fitting all the observed microwave transitions. The potential energy curve following this internal motion is reproduced in Figure 1. H_2O-CO_2 was also studied in N_2 and Ne matrices in the THz, far- and mid-infrared regions [6][7][8]. In particular Andersen *et al.* [8] reported the observation of three intermolecular bands however all at energies above 100 cm^{-1}. Finally, two rotationally resolved infrared spectra were reported. The first is due to Block and Miller [9]. They used a pulsed supersonic expansion for the production of the complex and the combination of a color centre laser and an optothermal detector to record the spectrum. This work was focused on the 1 OH stretch excitation (001) of the water entity, in the 3 μm spectral range. They estimated a value of 0.1356(13) cm^{-1} for the tunneling splitting corresponding to a barrier height of 305 cm^{-1} thus close to the value of Columberg *et al.* [5] previously mentioned. The tunneling splitting was assumed to be independent of the vibrational excitation. More recently, Zhu *et al.* [10] studied the same complex around the (010) state of water for both H_2O-CO_2 and D_2O-CO_2. They evaluated a variation of 5% of the tunneling splitting compared to the value of Miller and coworkers [9]. This complex has been also largely studied theoretically. In particular Sadlej and Makarewicz [11] first evaluated a complete potential energy surface using MP2 methods and a small but optimised basis set. More recently, in 2017, Wang and Bowman [2] calculated the complete potential energy surface using CCSD(T)-F12b/aug-cc-pVTZ level of approximation. The authors performed anharmonic evaluation of the intermolecular vibrational frequencies. Wang and Bowman also considered clathrate formation, predicting the structure of larger CO_2 hydrated complexes based on their two-body potential.

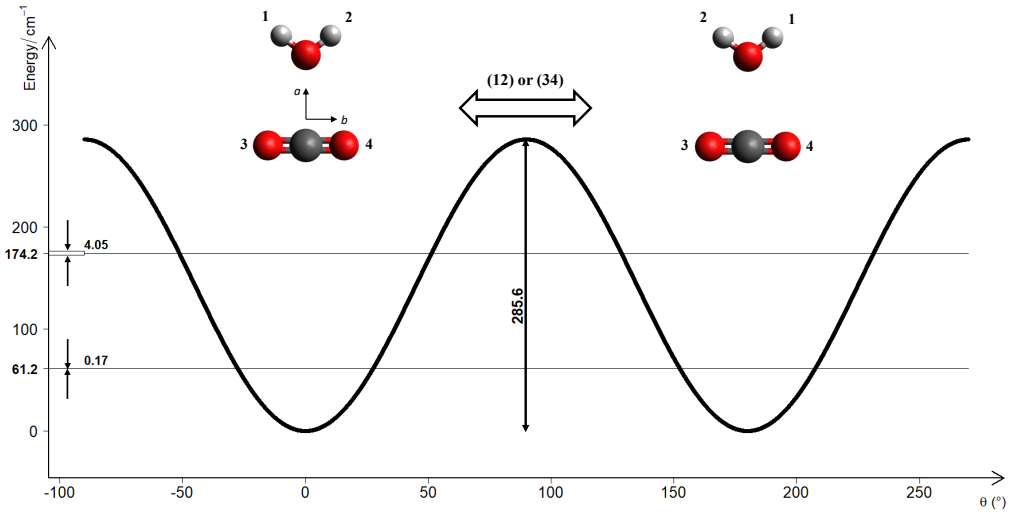

Figure 1. Potential energy curve and first energy levels (v = 0 and v = 1) for internal rotation (θ in deg) in H_2O-CO_2. The permutation operation (12) is pictured on top. Permutation (34) leads to the same result. Relevant nuclei are numbered. The barrier height (285.6 cm^{-1}) is from Columberg *et al.* [5]. The internal rotation splittings as calculated from the potential (see text) are indicated (not on scale). All energy values are in cm^{-1}.

The present report extends the high-resolution spectroscopic investigation of the H_2O-CO_2 complex with two quanta of excitation of the OH stretch *i. e.*, 2OH. The manuscript is structured as follows: Section 2 presents briefly the experimental setup, section 3 introduces the H_2O-CO_2 van der Waals complex and the molecular symmetry group used to assign the recorded spectrum, section 4 presents the overall spectrum and the results of the rotational analysis, section 5 focusses on the vibrational assignment and section 6 discusses the results, followed by concluding remarks in section 7.

2. Experiments

We used the FANTASIO+ (for "Fourier trANsform, Tunable diode and quAdrupole masS spectrometers Interfaced to a supersOnic expansion") setup [12][13], to investigate a supersonic expansion with water ("ultrapure" Milli-Q water with a resistivity of 18.2 MΩ cm), CO_2 (Air Liquide) and argon (Air Liquide) as a carrier gas. The main setup and bubbling injection procedure were as described in [14]. About 0.2 slm (liter per minute at standard conditions for temperature and pressure) of CO_2 and 4.4 slm of argon were injected in the supersonic expansion, so that constant reservoir (p_0) and residual (p_∞) pressures of 70 kPa and less than 2 Pa, respectively, were obtained. H_2O was seeded into the gas stream by passing about 5% of the carrier gas through the 30 cm long bubbler filled with liquid H_2O. The gas line and the nozzle were kept at room temperature. Concerning the cavity ringdown spectrometer, the cavity was composed of two concave mirrors (Layertec 109204, radius = 1000 mm, reflectivity = 99.999%). The ring-down time was typically around 190 μs. This corresponds to a 1 km effective absorption path length in the jet-cooled molecules downstream of the 1 cm long and about 12 μm wide slit. To increase the ring-down event rate, the same tracking circuit as previously reported [15] was used allowing typically some 150 ring-downs per spectral point to be recorded in less than 1.5 s. It yielded to an $\alpha_{min} = 5.10^{-10}$ cm^{-1} (considering the full length of the cavity as an effective absorption path length), where α is the absorption coefficient as defined in the work of Herman *et. al.* [12] it corresponds to a noise equivalent absorption (NEA) of 3.10^{-10} $cm^{-1}Hz^{-1/2}$. The sensitivity of the setup was limited by the photosensitivity of the InGaAs PIN photodiode (Hamamatsu G8376 − 03) in the transimpedance circuit monitoring the ring-down events. The spectrum was recorded with a resolution of about 4.10^{-4} cm^{-1}. Line positions were calibrated to better than 0.001 cm^{-1} using spectral lines of the jet-cooled water monomer with wavenumbers from HITRAN [16]. The rotational temperature (T_{rot}) was found to be 12 K from the distribution of the relative intensities in the rotational structure of the observed bands. Two DFB laser diodes: (10 mW, 1 MHz line width) were available for the experiment restricting the investigated range to the 7225 to 7260 cm^{-1} region.

3. The H_2O-CO_2 van der Waals complex

Due to the relative motion of the H_2O and CO_2 units, the complex needs to be considered in the G_8 molecular symmetry group. The character table we used is presented in Table 1 and is adapted from Ref [5].

A reasonable starting point of the spectral analysis is to consider the rotational (rot), vibrational(v), internal rotation (ir), electronic (e), nuclear spin (ns) and electronic spin (es) degrees of freedom as decoupled. One can then write the total

Table 1. characters of the irreducible representations for the G_8 molecular symmetry group .

G_8	E	(12)(34)	E*	(12)(34)*	(12)	(34)	(12)*	(34)*	$\|K_aK_c>$	ψ
A_1'	1	1	1	1	1	1	1	1	ee	$\psi_{(200)}^{H_2O}$,ψ_{ir}^{lower}, ψ_{ns}^{ortho} ψ_{vgs},ψ_e
A_2'	1	1	-1	-1	1	1	-1	-1	eo	
B_1'	1	-1	-1	1	1	-1	-1	1	oo	
B_2'	1	-1	1	-1	1	-1	1	-1	oe	
A_1"	1	1	1	1	-1	-1	-1	-1		ψ_{ir}^{upper}
A_2"	1	1	-1	-1	-1	-1	1	1		
B_1"	1	-1	-1	1	-1	1	1	-1		ψ_{tot}
B_2"	1	-1	1	-1	-1	1	-1	1		ψ_{tot},$\psi_{(101)}^{H_2O}$,ψ_{ns}^{para}, $\psi_{v_3odd}^{CO_2}$

wavefunction as:

$$\psi_{tot} = \psi_{ns}\psi_{ir}\psi_{rot}\psi_v\psi_e\psi_{es} \quad (1)$$

Where ψ_{tot} of H_2O-CO_2 must comply with the Pauli principle. It thus corresponds to B_1" or B_2" irreducible representations. As shown in Table 1, ψ_e and ψ_{es}, ψ_{vgs} (for the vibrational ground state) and $\psi_{(200)}^{H_2O}$ are of A_1' symmetry, while $\psi_{(101)}^{H_2O}$ is B_2" [9]. The H_2O-CO_2 van der Waals complex is an asymmetric top. The irreducible representation of ψ_{rot} is solely determined by the parity of K_a and K_c, *i. e.* the projections of the total angular momentum J onto the a and c axes of inertia, respectively. The irreducible representations associated to each set of parity of K_a and K_c, noted 'e' for even and 'o' for odd, are provided in Table 1. For the ground vibrational state the combination of the different components of the total wavefunction and the Pauli requirement leads to the existence of only one tunneling component per rotational level. The K_a parity determines the spin statistical weight. This is illustrated in Figure 2. As discussed in the next section, the two vibrational bands observed in this work show b-type structure indicating a B_2" vibrational symmetry for each of the upper states. Upper state symmetry labels in Figure 2 correspond to this B_2" vibrational symmetry and indicated energies are associated to one of the observed states, that assigned to the (101) vibrational state of H_2O.

4. Rotational analysis

Figure 4 presents the experimental spectrum and the associated rovibrational simulation. All simulations in this work were performed using the Pgopher software [17]. The explored spectral range is that of (101) in H_2O. The corresponding excitation in the complex is thus expected to lead to a b-type band (*i. e.* with ΔK_a=odd and ΔK_c=odd). Surprisingly two bands can be identified with origins close to 7238 and 7247 cm^{-1}. They are labelled I/II, respectively on the Figure 4 and in the text hereafter. The two bands are simulated in Figure 4 (bottom part), using the constants from the present results.

The energy levels for all vibrational states were calculated using Watson Hamiltonians in A reduction [20]. This Hamiltonian is implemented in the Pgopher software. As previously mentioned this complex presents large amplitude relative motion of the

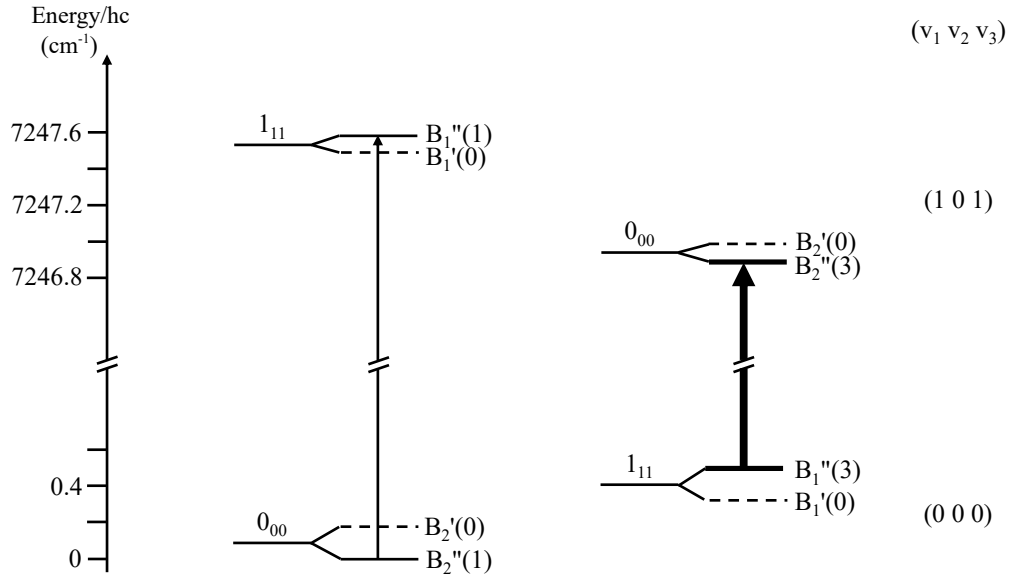

Figure 2. The first two rotational levels ($J_{K_a K_c}$) of the H_2O-CO_2 complex, their associated internal rotation splittings and the irreducible representation of ψ_{tot} are presented for the ground and (101) vibrational levels in H_2O. Statistical weights are indicated between parentheses for each level. Those with 0 values are in dashed line. Transitions obeying *b*-type selectrion rules are drawned unsing vertical lines.

Table 2. Spectroscopic parameters for the H_2O-CO_2 van der Waals complex. Uncertainties in parentheses are 1σ from the least-squares fits.

Vibrational state	Ground state[a]		(101)		(200)+ ν_{12}	
Spectroscopic constants	K_a *even*	K_a *odd*	K_a *even*	K_a *odd*	K_a *even*	K_a *odd*
ν_0/cm^{-1}			7246.89465(14)	7247.08945(11)	7237.53892(27)	7237.66352(17)
A/MHz	11514.723	11501.23	11555.99(33)	11556.74(24)	11633.89(99)	11621.94(51)
B/MHz	4674.4133	4675.07856	4649.57(19)	4652.05(15)	4644.69(35)	4642.79(25)
C/MHz	3304.3476	3304.61774	3286.94(14)	3290.62(15)	3277.55(43)	3277.04(24)
D_{JK}/MHz	0.334239		0.3210(41)	0.455(11)	0.2441(65)	0.3163(83)
D_J/MHz	0.028388		0.02093(90)	0.03260(77)	0.0419(20)	0.0267(21)
D_K/MHz	-0.32		-0.240(10)	-0.2927(85)	-0.245(28)	-0.241(12)
δ_K/MHz	0.23317		0.23317[b]		0.23317[b]	
δ_J/MHz	0.008459		0.008459[b]		0.008459[b]	
σ/MHz			15		21	

[a] Ground state rotational constants were fixed to the values determined by microwave spectroscopy in Ref [5].

[b] Constrained from the ground state.

two molecules leading to a tunneling splitting of all rovibrationnal levels. There is no sign of nuclear spin relaxation in the present spectrum. Since each parity of K_a is associated to a tunnelling component and a nuclear spin isomer, the two different tunneling components are dealt with two different molecules. Two molecules with 1:3 abundance ratio were thus considered in the analysis.

226 lines were assigned for band II (7238 cm^{-1}) and 259 lines for the band I (7247 cm^{-1}). All assignments for lines with $J < 6$ and $K_a < 5$ were verified using combination differences from the work of Columberg *et al.* [5]. The rotational constants are presented in Table 2. Although not all observed lines are accounted for in the analysis, the agreement between simulated and observed spectra is satisfactory for band I. Severe perturbations were observed for band II, in particular, for the $K'_a - K_a$" 0-1 subband which presents an irregular pattern in terms of intensity namely for the

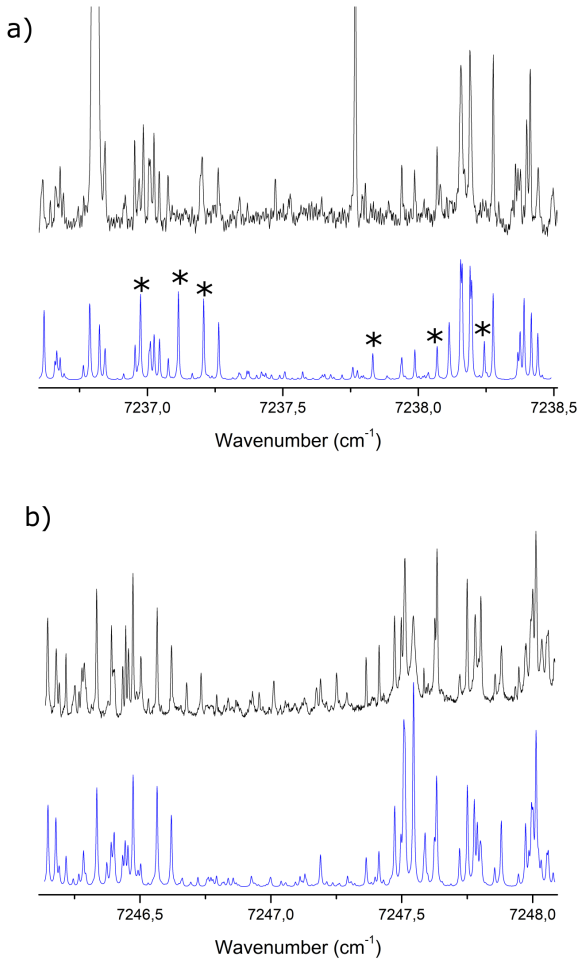

Figure 3. Observed (top) and simulated spectra (bottom) of H_2O-CO_2 in the vicinity of the band origin of bands II (a) and I (b). * denotes perturbed lines discussed in the text.

$J' = 2$ to $J' = 4$, as illustrated by asteriks in Figure 3. One should, however notice that these local perturbations are consistent for P/Q/R lines with the same upper rotational level. Their origin remain unassigned.

5. Vibrational assignment

Two bands (I and II with origins at 7238 and 7247 cm^{-1} respectively) are observed in the studied range. Their origins are thus separated by some 9 cm^{-1}. As demonstrated by the rotational analysis, both bands are of *b*-type. The rotational constants for the two upper states, as presented in Table 2, appear to be very similar. As detailed in this Table and previously, perturbations are more numerous in Band II, and the fit in Band II presents a standard deviation twice as large as in Band I. It was also already mentioned that, although few perturbations affecting P/Q/R lines with the same upper rotational level can be clearly identified for both bands, at low J values in particular, the agreement with the calculated spectrum appears not to be fully

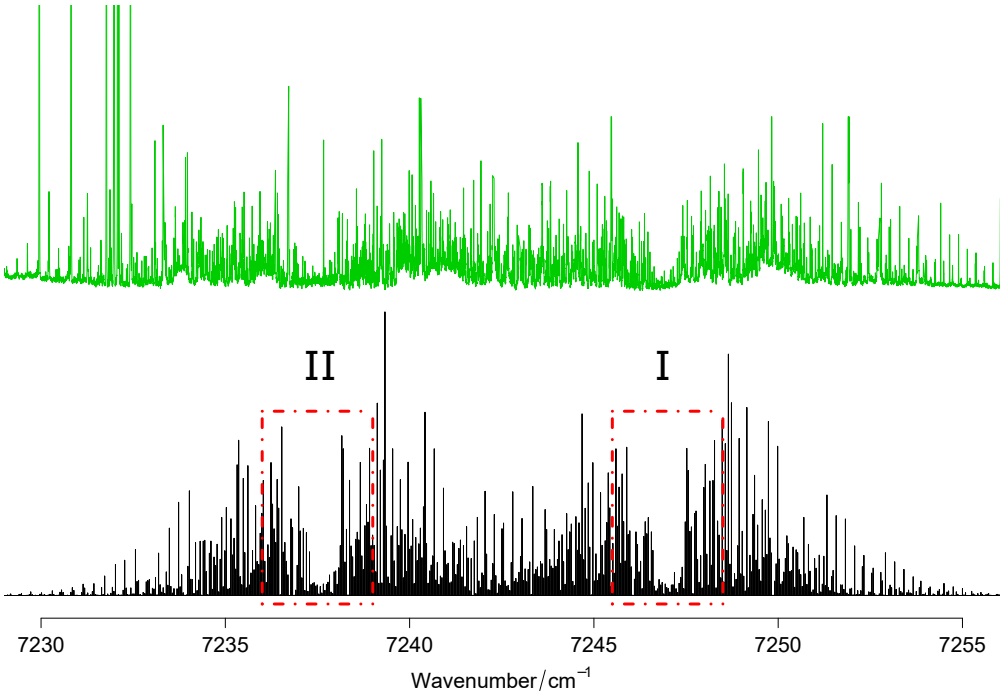

Figure 4. Overall experimental spectrum (top), strong lines due to H_2O-Ar (see [18]) and H_2O-H_2O (see [19]) dimer are also observed but not highlighted on the Figure. The associated simulation of bands I and II from the present results are shown with two dashed rectangle outlining the position of the two bands origin.

satisfactory for band II while it is very convincing for band I as illustrated in Figure 5. A last piece of information is that both bands present very similar intensities, with band I about 10 % stronger than band II, as appearing in Figure 4. The recent investigation H_2O-Ar/Kr in the 2OH excitation range using the same set-up and very similar experimental conditions, Refs [18] and [21], also demonstrated the presence of two main bands. They were assigned to excitation to the upper ($v_1v_2v_3$)= (200) and (101) vibrational levels in H_2O, with monomer energies at 7201.540 and 7249.817 cm^{-1} respectively. The same assignments can, however, not be claimed here for bands I and II in H_2O-CO_2. Indeed, *a*- (to (020)) and *b*- (to (101)) type bands are observed in H_2O-Ar/Kr while both bands are of *b*-type in the present case. Furthermore, the spacing between the bands for H_2O-Ar/Kr, that is close to that between (200) and (101) vibrational levels in H_2O, *i. e.* about 48 cm^{-1}, is here reduced to only 9 cm^{-1}. Also, besides a strong local perturbation that was observed and analyzed in H_2O-Ar[18], the rotational structure is very regular and nicely reproduced by the simulation using an asymmetric top rotor Hamiltonian for the complex with Ar/Kr, while one of the bands (band II) presently investigated presents sharp disagreement with the simulation at higher K/J values.
Actually, band I with the expected band-type (*i. e. b*-type), is close to the expected origin (red shift of 3 cm^{-1}) and shows regular rotational structure, can be readily assigned to excitation of the (101) upper state in H_2O.

The problem thus arises with band II, with origin at 7238 cm^{-1}. It cannot be assigned to excitation of the (200) in H_2O. Indeed, it demonstrates a different (*b*–

instead of $a-$) band type, the band origin is too far shifted to blue ((200) is at 7202 cm^{-1} *i. e.* 45 cm^{-1} lower in energy than Band II) and the rotational structure doesn't agree with that of a conventional asymmetric top. Before discussing the vibrational assignment of band II, it should be recalled that the range presently studied is instrumentally limited from 7225 to 7260 cm^{-1}. Transition to (200) (7202 cm^{-1}) with a full breath similar to that of band I (*i. e.* about 15 cm^{-1}, see Figure 4) therefore falls outside the presently investigated range. There is actually no reason that transition to (200) in H_2O-CO_2 should not be observed under appropriate instrumental conditions, which we hope to gather in the future.
Although the rotational structure in band II is not ideally reproduced by the asymmetric rotor Hamiltonian the detailed pattern and the low J/K lines satisfactorily agree with this model. The rotational constants retrieved from the fit are thus somewhat meaningful. Their close similarity with those of band I therefore excludes the possibility that another molecular complex, including one of the $(H_2O)_n$-$(CO_2)_m$ type as reported in the literature [6], is the carrier of band II.
One could invoke vibrational excitation in CO_2 rather than in H_2O for band II. For symmetry reasons, see Table 1, the related level should then carry odd excitation in the CO_2 asymmetric stretch. Figure 6 depicts the exhaustive set of relevant H_2O and CO_2 vibrational levels. It shows that only one CO_2 level with adequate symmetry, vib= (4001) at 7284 cm^{-1}), is present in the 1.4 μm investigated range, however at some 40 cm^{-1} above the observed band origins. In addition the related transition band strength is too weak to lead to an observable spectrum of any related molecular complex given the S/N performances of FANTASIO. One should therefore only consider excitation in H_2O for band II.

Given that only two vibrational levels in H_2O are relevant, as appearing in Figure 6, the only possible assignment for band II must involve (200) and an intermolecular mode ν_{int} in H_2O-CO_2. Considering no vibrational shift, the mode frequency must be around 36 cm^{-1} and have B_2'' symmetry, to comply with the band origin and the observed band type, respectively. Intermolecular modes in H_2O-CO_2 were reported from matrix investigation, however with the frequencies of the order of or higher than 100 cm^{-1} [8]. Fortunately *ab initio* calculations by Wang and Bowman recently provided a complete set of predictions [2]. The frequency of the lowest energy intermolecular mode, ν_{12}, is calculated to be 34 cm^{-1}, thus close to the required value (36 cm^{-1}). It has the required B_2'' symmetry, thus leading to a b-type band when combined with the totally symmetric (200) level. The next, higher energy intermolecular mode with adequate symmetry, ν_{11}, is calculated at 178 cm^{-1}, that would lead to a combination band origin around 7380 cm^{-1}, thus too high compared to the observed value (7238 cm^{-1}). For completeness, it should be mentioned that additional combinations involving (021) in H_2O (not shown in Figure 6) were calculated, all leading predicted band origins differing by more than 200 cm^{-1} from the observed value.

We are therefore confident that band II corresponds to the transition from the ground state to the combination level (200) of H_2O + ν_{12} (intermolecular). The contribution of off diagonal anharmonicity (x_{ij}) to the level energy and therefore to the band origin has been neglected here above. We do indeed expect $x_{1,12}$ to be very small, typically 1% of the lowest frequency mode, thus less than 1 cm^{-1}[22]. The ν_{12} mode frequency is then found to be the difference between the origin of band II and the position of (200) in the complex. Considering an identical red shift (of 3 cm^{-1}) for (101) and (200) in the complex, the ν_{12} mode frequency is estimated to be 39 cm^{-1}.

The last puzzle with band II assignment is the band intensity. It is similar to that of band I. Similar band strengths are expected for transitions leading to (200) and (101), as reported for H_2O-Ar/Kr [18][21]. This is not expected to occur for bands I and II since combination with an intermolecular mode is involved in band II that, in principle should lead to a significantly weaker band than excitation to (101) (band I). Previous results for other molecular complexes, such as C_2H_2-N_2O also observed in the overtone range using FANTASIO [23], confirm that the relative band strength should be in favor of the main overtone excitation. A probable explanation of the similar band intensities is that intensity sharing between transitions I and II occurs thanks to a Fermi type anharmonic resonance coupling (101) and (200) $+\nu_{12}$. Such resonances were already reported in C_2HD-Ne [24]. The role of the Fermi resonance on the band origins is probably very small since the band origin of (101) in H_2O-CO_2 is very close to that expected (shift of only 3 cm^{-1} compared to (101) in H_2O), as expected in the absence of Fermi-type resonance.

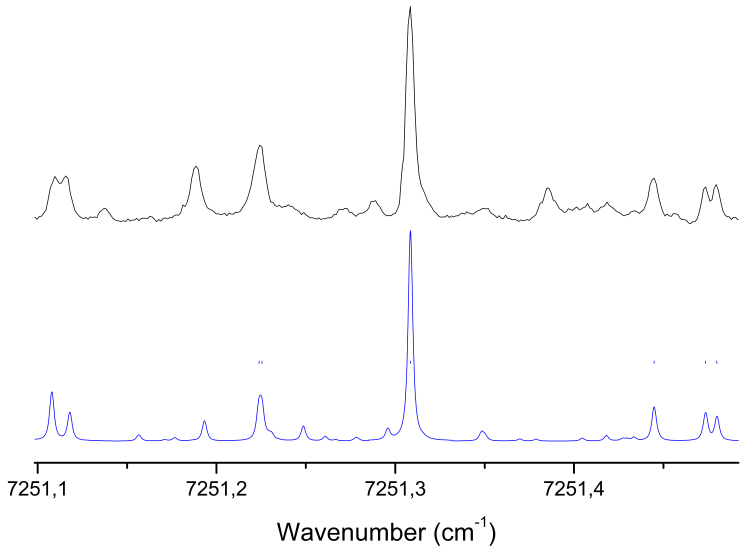

Figure 5. Observed (top) and simulated spectra (bottom) of H_2O-CO_2 on the blue side of band I.

6. Results

6.1. Tunnelling dynamics

Hereafter we denote by S'' and S' the splitting of each rotational level in the vibrational ground state and excited vibrational states, respectively. As illustrated in Figure 7 a combination of the band origins within each K_a parity can be used to retrieve a sum/difference of S'' and S' for *b-/a-* type bands. The value of S''=0.1356 cm^{-1} from Ref [9] can be used to estimate trends in S'. Correcting a typo in [9], *i. e.* swapping the two band origins in their Table II, and compiling data from this study and the

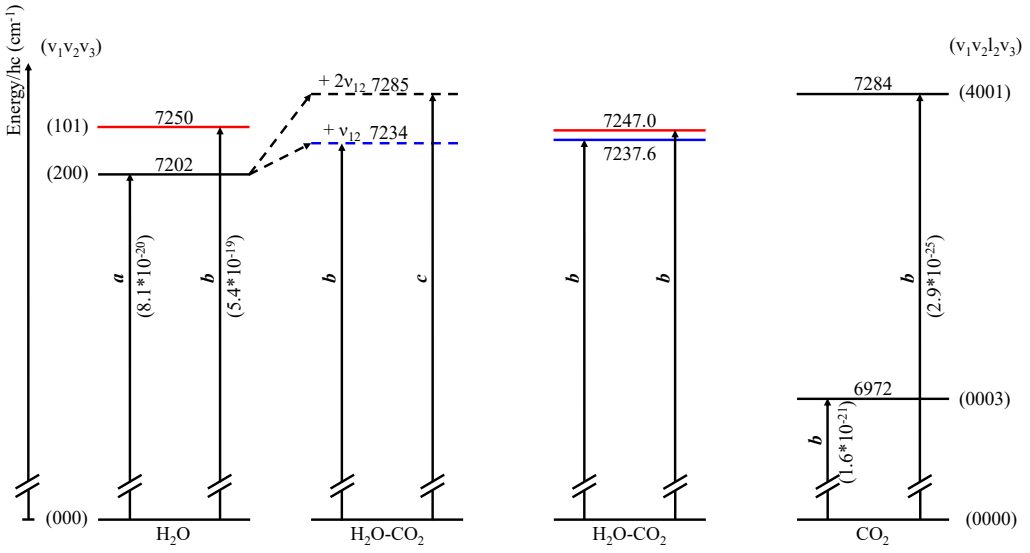

Figure 6. Observed vibrational levels in H_2O-CO_2 and relevant ones in isolated CO_2 and H_2O. The Figure includes a combination level in H_2O-CO_2 involving (200) in H_2O and an intermolecular vibrational mode as predicted from *ab initio* calculations by Wang and Bowman [2]. Color lines help identifying matching levels. All expected (*a*- and *b*-) band-types from the ground state are indicated. Related transition band intensities, in $cm^{-1}/\left(\text{molecule}.cm^{-2}\right)$, from the ground state are indicated for the isolated species. These values and the level labels are from [16]. Energy levels with their vibrational assignment (and absorption cross-section) of the CO_2 and H_2O moieties in the spectral range covered in this work. This figure includes also as a dashed line the sum of (200) of H_2O and the prediction of an intermolecular mode from Wang and Bowman[2].

literature, S' was evaluated for the various vibrational excited states investigated, as gathered in Table 3. These results indicate a large sensitivity of intermolecular tunnelling dynamics with intramolecular vibrational excitation. It is interesting to point out that the splitting decreases with the number of quanta of vibrational excitation. Finally, (200)+ν_{12} shows a change of sign of S' and thus a change in the ordering of the tunnelling components. The specificity of the rotational structure in this level is further commented on later in this section.

Table 3. Summary of the tunnelling splittings in cm^{-1} for the H_2O-CO_2 van der Waals complex.

Vibrational state	$\Delta\nu_0 = \nu_0(Ka'' = even) - \nu_0(Ka'' = odd)$	Splittings combination	S' considering S"=0.1356(13)cm^{-1} [b]
$(010)^a$	0.0070(2)	S"-S'	0.129(2)
$(001)^b$	0.268(1)	S"+S'	0.133(1)
$(101)^c$	0.1948(3)	S"+S'	0.059(2)
$(200)+\nu_{12}^c$	0.1246(5)	S"+S'	-0.011(2)

[a] from Ref [10].

[b] from [9].

[c] this work.

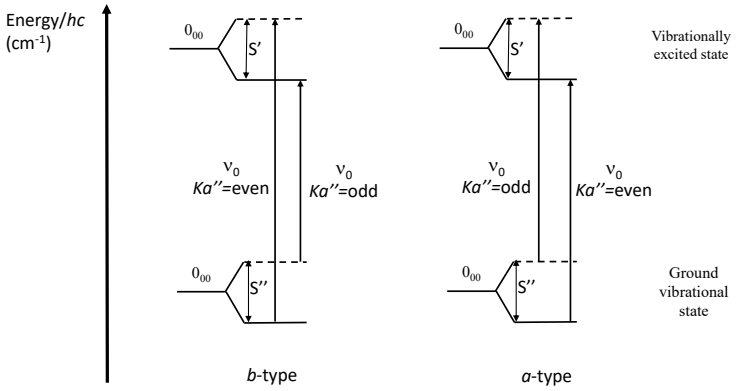

Figure 7. Energy level diagram in H_2O-CO_2 showing upper and lower state tunnelling splittings of the rotational, JK_aK_c, energy levels for the various case studies. Band origins (ν_0) for Ka'' odd and even are indicated by vertical arrows.

6.2. Rotational perturbations in band II

As previously mentioned, the low J/K lines in band II show very good agreement with asymmetric rotor Hamiltonian modeling. Local perturbations are clearly identified from inspection of lines with low J/K values. Given the low density of isolated water vibrational levels and given the fact that the intermolecular mode in band II is the lowest frequency one, these local perturbations must arise from interaction with higher K states in (200) H_2O. One can, however not exclude that the perturbation mechanism involves another intermolecular mode of different symmetry that would lie only very slightly higher than ν_{12}. Mode ν_8 (B_1) calculated at 75 cm^{-1} by Wang and Bowman is a possible candidate. Other combination of a larger number of modes could also be considered as possible candidates. It is interesting to point out that higher J/K lines are only approximately reproduced using the asymmetric rotor model. Similar problems were encountered when dealing with combination bands involving intermolecular modes in C_2H_2-Ar [25]. These were partly solved using more appropriate models, as the use of intermolecular potential energy surface and solving the nuclear Schrödinger equation, to better describe the intermolecular large amplitude motion [26]. We hope to similarly later reconsider the rotational structure of band II in H_2O-CO_2.

6.3. Lifetime in the excited state

By constraining the Doppler component of the observed lineprofile on the spectrum to a Voigt profile calculated using T_{rot} = 12 K, one can evaluate the Lorentzian contribution to the profile and estimate the vibrational predissociation lifetime in each rovibrational state. This procedure was achieved in all previous investigations using FANTASIO+ [12] as summarized in [23]. It assumes an equivalent translational and rotational temperatures. A lifetime of the order of 1 ns can then be retrieved. It is identical for both observed vibrational levels. It is, as expected, shorter than that

reported for ν_3 by Miller and co-workers [9] (100 ns $< \tau <$ 200 μs). Compared to other water-containing molecular complexes species studied in the 2OH overtone range with the same instrument, the lifetime of H_2O-CO_2 is similar but slightlty shorter (see Table 3 in Ref [27] for detailed comparison). Some of the previous studied species showed rotational dependence in the vibrational predissociation lifetime. This is not the case for H_2O-CO_2 since all the rotational lines present a very similar linewidth.

7. Summary and conclusions

Two rovibrational bands were observed in the region of the (101) band of H_2O using cavity ring-down spectroscopy in a supersonic jet of a mixture consisting of water, carbon dioxide and argon, in the region between 7225 and 7260 cm^{-1}. One of them is assigned to the (101) excitation of the H_2O unit in the H_2O-CO_2 molecular complex and the other band is assigned to the (200)+ an intermolecular mode excitation. This intermolecular mode is the lowest frequency one, having a B_2'' symmetry. This mode is predicted by *ab initio* calculations to be at 32 cm^{-1} close to the 39 cm^{-1} experimental value obtained in this work. By an inspection of the results obtained in this study and the compilation of previous published works it is clear the tunneling dynamics appears to be significantly impacted by intramolecular excitation nature and frequency. Finally, vibrational predissociation lifetime in both observed upper states is determined from the experimental linewidths to be of the order of 1 ns. It is identical for all upper rotational levels. We hope to observe the missing (200) band in the complex and therefore definitely confirm our vibrational assignment by extending the instrumental capacity of the experimental setup in a future investigation.

8. Acknowledgements

C. L. thanks the financial support of the Fonds de la recherche scientifique-FNRS under grant number J.0179.18 (CDR-Sensitive Optical Spectroscopy at 20K) and the Action de Recherches Concertées (ARC Ibeam-18/23-090). The authors are indebted to the Service de "Chimie Quantique et Photophysique" of the "Université libre de Bruxelles" for the loan of the FANTASIO set-up.

9. References

References

[1] G.M. Chaban, M. Bernstein and D.P. Cruikshank, Icarus **187** (2), 592–599 (2007).
[2] Q. Wang and J.M. Bowman, The Journal of Chemical Physics **147** (16), 161714 (2017).
[3] Y. Park, D.Y. Kim, J.W. Lee, D.G. Huh, K.P. Park, J. Lee and H. Lee, Proceedings of the National Academy of Sciences **103** (34), 12690–12694 (2006).
[4] K. Peterson and W. Klemperer, The Journal of Chemical Physics **80** (6), 2439–2445 (1984).
[5] G. Columberg, A. Bauder, N. Heineking, W. Stahl and J. Makarewicz, Molecular Physics **93** (2), 215–228 (1998).
[6] P. Soulard and B. Tremblay, The Journal of Chemical Physics **143** (22), 224311 (2015).
[7] X. Zhang and S.P. Sander, The Journal of Physical Chemistry A **115** (35), 9854–9860 (2011).

[8] J. Andersen, J. Heimdal, D. Mahler, B. Nelander and R.W. Larsen, Communication: THz absorption spectrum of the CO2–H2O complex: Observation and assignment of intermolecular van der Waals vibrations AIP 2014.
[9] P. Block, M.D. Marshall, L. Pedersen and R. Miller, The Journal of Chemical Physics **96** (10), 7321–7332 (1992).
[10] Y. Zhu, S. Li, P. Sun and C. Duan, Journal of Molecular Spectroscopy **283**, 7–9 (2013).
[11] J. Sadlej, J. Makarewicz and G. Chałasiński, The Journal of Chemical Physics **109** (10), 3919–3927 (1998).
[12] M. Herman, K. Didriche, D. Hurtmans, B. Kizil, P. Macko, A. Rizopoulos and P.V. Poucke, Molecular Physics **105** (5-7), 815–823 (2007).
[13] K. Didriche, T. Földes, C. Lauzin, D. Golebiowski, J. Liévin and M. Herman, Molecular Physics **110** (21-22), 2781–2796 (2012).
[14] K. Didriche and T. Földes, The Journal of Chemical Physics **138** (10), 104307 (2013).
[15] T. Földes, Review of Scientific Instruments **84** (1), 016102 (2013).
[16] I.E. Gordon, L.S. Rothman, C. Hill, R.V. Kochanov, Y. Tan, P.F. Bernath, M. Birk, V. Boudon, A. Campargue, K. Chance *et al.*, Journal of Quantitative Spectroscopy and Radiative Transfer **203**, 3–69 (2017).
[17] C.M. Western and B.E. Billinghurst, Physical Chemistry Chemical Physics (2019).
[18] T. Vanfleteren, T. Földes, M. Herman, J. Liévin, J. Loreau and L.H. Coudert, The Journal of Chemical Physics **147** (1), 014302 (2017).
[19] N. Suas-David, T. Vanfleteren, T. Foldes, S. Kassi, R. Georges and M. Herman, The Journal of Physical Chemistry A **119** (39), 10022–10034 (2015).
[20] J.K. Watson, Vibrational spectra and structure (Ed: J. Durig) Elsevier: Amsterdam 1977.
[21] T. Vanfleteren, T. Földes, A. Rizopoulos and M. Herman, Journal of Molecular Spectroscopy **342**, 92–99 (2017).
[22] N. Moazzen-Ahmadi and A. McKellar, International Reviews in Physical Chemistry **32** (4), 611–650 (2013).
[23] M. Herman and D.S. Perry, Physical Chemistry Chemical Physics **15** (25), 9970–9993 (2013).
[24] R. Bemish, L. Oudejans, R. Miller, R. Moszynski, T.G. Heijmen, T. Korona, P.E. Wormer and A. van der Avoird, The Journal of Chemical Physics **109** (20), 8968–8979 (1998).
[25] C. Lauzin, K. Didriche, P. Macko, J. Demaison, J. Liévin and M. Herman, The Journal of Physical Chemistry A **113** (11), 2359–2365 (2009).
[26] C. Lauzin, L.H. Coudert, M. Herman and J. Liévin, The Journal of Physical Chemistry A **117** (50), 13767–13774 (2013).
[27] M. Herman, T. Földes, K. Didriche, C. Lauzin and T. Vanfleteren, International Reviews in Physical Chemistry **35** (2), 243–295 (2016).